



Hydro-geomorphological modelling of leaky wooden dam efficacy from reach to catchment scale with CAESAR-Lisflood 1.9j

5 Joshua M. Wolstenholme^{1,2}, Christopher J. Skinner^{3,2}, David Milan⁴, Robert E. Thomas² and Daniel R. Parsons¹

¹Geography and Environment, Loughborough University, Loughborough, UK

²Energy and Environment Institute, University of Hull, Hull, UK

³FloodSkinner, UK

⁴School of Environmental Sciences, University of Hull, Hull, UK

10 *Correspondence to:* Joshua M. Wolstenholme (j.m.wolstenholme@lboro.ac.uk)

Abstract. Leaky wooden dams are woody structures installed in headwater streams that aim to reduce downstream flood risk through increasing in-channel roughness and decreasing river longitudinal connectivity in order to desynchronise flood peaks within catchments. Hydrological modelling of these structures omits sediment transport processes since the impact of these processes on flow routing is considered negligible in comparison to in-stream hydraulics. Such processes are also excluded on the grounds of computational expense. Here we present a study that advances our ability to model leaky wooden dams through a roughness-based representation in the landscape evolution model CAESAR-Lisflood, introducing a flexible and representative approach to simulating the impact of leaky wooden dams on reach and broader catchment-scale processes. The hydrological and geomorphological sensitivity of the model is tested against grid resolution as well as a variability in key parameters such as leaky dam gap size and roughness. The influence of these parameters are also tested in isolation from grid resolution, whilst evaluating the impact of simulating sediment transport on computational expense, model domain outputs and internal geomorphological evolution. The findings show that simulating sediment transport increased the volume of water stored in the test reach by up to an order of magnitude whilst reducing discharge by up to 31% during a storm event. We demonstrate how this is due to the leaky dam acting to induce geomorphic change and thus increasing channel roughness. When considering larger grid resolutions, however, our results show that care must be due to overestimations of localised scour and deposition in the model and that behavioural approaches should be adopted when using CAESAR-Lisflood in the absence of robust empirical validation data.

1. Introduction

30 Natural flood management (NFM) seeks to emulate natural processes to reduce flood risk through the attenuation of water, ‘slowing the flow’ by desynchronising tributaries, reducing surface runoff and/or improving channel-floodplain connectivity (SEPA, 2015; Burgess-Gamble et al., 2017; Lane, 2017). NFM is becoming increasingly popular with flood risk managers due to its multiple benefits and perceived low risk, as well as its ability to engage local communities and land users in potentially reducing flood risk (Burgess-Gamble et al., 2017; Dadson et al., 35 2017; Newson et al., 2021). Reintroduction of wood to the river channel is a popular form of NFM, employed for multiple co-benefits such as habitat creation, ecological enhancements as well as river engineering, and



downstream flood hazard reduction. As a result NFM now accounts for approximately 20% of UK river restoration projects (Cashman et al., 2018; Grabowski et al., 2019).

40 One method of introducing wood is through building leaky wooden dams (LDs). LDs are a form of in-channel blockage that can be installed either within a river channel (Metcalf et al., 2017; Deane et al., 2021) or, as a runoff attenuation feature (RAF), intersecting surface runoff pathways (Nicholson et al., 2012; Nicholson et al., 2019) in an effort to reduce slow flows and reduce flood risk, increase biodiversity, and improve river heterogeneity (Burgess-Gamble et al., 2017). LDs aim to emulate natural woody debris found in river channels
45 by partially or completely blocking the channel to accelerate the recruitment of natural wood as part of the natural wood cycle (Gregory et al., 1985; Addy and Wilkinson, 2016). LDs have multiple benefits including (but not limited to): improving water quality, increasing habitat diversity, flood wave attenuation, and increasing floodplain connectivity (Wenzel et al., 2014; Burgess-Gamble et al., 2017; Grabowski et al., 2019).

50 Despite their rapid deployment in riverine management over recent years, a key knowledge gap is how LD efficacy evolves temporally, both in response to geomorphic evolution up- and downstream of the LD, but also in response to flood sequences (Addy and Wilkinson, 2019; Grabowski et al., 2019). Challenges in disentangling the relative impact of LDs from the influence of land use, antecedent conditions and other flood risk management interventions presently result in an unclear understanding of their influence over time. Recent works have focused
55 on integrating LDs into 1D and 2D models at different spatial scales (Hill et al., 2023), most commonly representing the interventions as localised roughness adjustments (Pinto et al., 2019), geometry adjustments (Pearson, 2020; Walsh et al., 2020), or a combination of the two (Dixon et al., 2016; Senior et al., 2022). LDs have also been represented in hydraulic models, through stage-discharge relationships realising LDs (and other RAFs) as weirs or culverts (Thomas and Nisbet, 2012; Metcalf et al., 2017; Keys et al., 2018; Hankin et al.,
60 2019; Pinto et al., 2019; Hankin et al., 2020; Leakey et al., 2020; Pearson, 2020). A comprehensive review of the large wood numerical modelling literature focused on artificially placed wood can be found in Addy and Wilkinson (2019).

The vast majority of numerical models used for LD evaluation have not considered the impacts of sediment
65 transport on function and efficacy. This is in-line with operational approaches to modelling flood risk, where sediment transport processes have often been considered as a negligible source of uncertainty (Flack et al., 2019). Despite this those models that solve only for the hydrodynamic component often produce erodibility maps (Hankin et al. 2019; Pearson, 2020), or report the cross-sectional- or depth-averaged velocity and shear stress components (Bair et al., 2019) on the bed and banks. However, many previous studies have focused on the reach-
70 scale, or small catchments (< 10 km²), simulating one or a small number of LDs (Addy and Wilkinson, 2019) in isolation. It is therefore difficult to validate results at larger scales, especially when combined with a greater range of flows, rarer high flow events and increased complexity (Metcalf et al., 2017). Those that have attempted catchment-scale simulations, such as the network model of Hankin et al. (2020), have not considered sediment transport in any of the scenarios explored. A few studies do exist that simulate sediment transport and riverine
75 geomorphic evolution in response to LDs. Walsh et al. (2020) used the landscape evolution model (LEM) CAESAR-Lisflood (Coulthard et al., 2013) to assess the impact on channel response and suspended sediment flux



of large wood in a small headwater catchment. Large wood was represented using the bedrock layer in CAESAR-Lisflood (i.e., an unerodable fixed bed) but such an approach does not represent LD function and does not permit the throughflow of water nor represent a lower gap to allow unimpeded passage of baseflows. Pearson (2020) also
80 used CAESAR-Lisflood to implement runoff attenuation and used an approach that features as edits LDs within the terrain. This method allowed features to be eroded, but again lacked porosity and a lower flow gap. As such, no work currently exists that incorporates both the inherent ‘leakiness’ of LDs and the ability to simulate a lower gap, sediment transport and longer-term geomorphic evolution. Here we address this methodological gap to advance substantive understanding. We present new NFM functionality for the CAESAR-Lisflood landscape
85 evolution model (Coulthard et al., 2013) which is capable of representing the restriction to flow due to LDs dynamically, i.e., the level of restriction varies based on the water level. This study utilises a virtual test bed, based on a prototype real-world location, in order to fully evaluate the ability of the model to simulate geomorphic response to LDs, whilst additionally comparing results to fixed-bed simulations. We present the advances of the LD modelling toolkits and demonstrate the ability to capture key processes. We additionally complete a sensitivity
90 analysis of the modelling solutions in order to demonstrate the robust simulation of a range of complex LD scenarios at both reach and catchment scale.

2. CAESAR-Lisflood

2.1. Model description

Geomorphic processes are complex, and consequently high-fidelity numerical models designed to simulate them
95 are also complex and computationally demanding, meaning long-term simulations (10–100s of years), or multiple simulations of different scenarios, can take substantial computational resources. Time is a barrier to decision makers who may wish to use information from simulations in order to plan flood management interventions and/or river restoration schemes. LEMs reduce complexity by simplifying processes, increasing computational efficiency and enabling useful and timely information to be extracted. Originally designed to investigate broad scale controls and behavioural changes to landscapes as they develop over long timescales (10^2 – 10^6 years), LEMs have been
100 key to a range of advances in the understanding of long-term geomorphic processes. Developments in computational power has increased the complexity of some LEMs whilst retaining their efficiency, leading to the development of ‘second generation’ LEMs such as CAESAR-Lisflood, herein referred to as CL. This has extended the capabilities of the original LEM for wider applications, including for example, landslide risk (Xie et al., 2022), hazards to electricity transmission towers (Feeney et al., 2022), mining (Hancock et al., 2017) and flood risk
105 management (Croke et al., 2016; Ramirez et al., 2020).

CAESAR-Lisflood is a second-generation LEM that merged the original CAESAR LEM with the 2D hydraulic code, Lisflood-FP (Bates et al., 2010), replacing the original simplistic steady-state hydraulic code (Coulthard et al., 2013). The development allows the model to simulate geomorphic processes at event-scale whilst retaining
110 its efficiency. Further developments within CL has enabled application in flood risk management through the ability to apply spatially distributed rainfall within the model domain, allowing for representation of convective events (Coulthard and Skinner, 2016). As such, CL is a suitable model to further enhance with new tools to simulate NFM approaches, such as LDs. CL can have one or more direct hydraulic source inputs that can be used



115 in both catchment and reach modes, in combination with rainfall. CL requires minimal data (elevation and rainfall
or a discharge input) for operation, uses readily available regular gridded DEM data with a range of grid sizes, is
open source and highly customisable, and crucially can simulate spatially distributed morphodynamic evolution
utilising up to nine grain size fractions (Meadows, 2014; Hancock et al., 2015; Pearson, 2020; Walsh et al., 2020).
Fluvial erosion and deposition are governed by three selectable sediment transport laws: Wilcock and Crowe
120 (2003), Einstein (1950) or Meyer-Peter and Müller (1948). As CL ingests a regular raster grid, attributes can be
assigned to each unique cell including roughness (Manning's n), TOPMODEL m value and more (Li et al., 2023).
Here, version 1.9j, first released in August 2019, is used as the baseline for development (available here
<https://sourceforge.net/projects/caesar-lisflood/files/>).

2.2. Leaky dam module

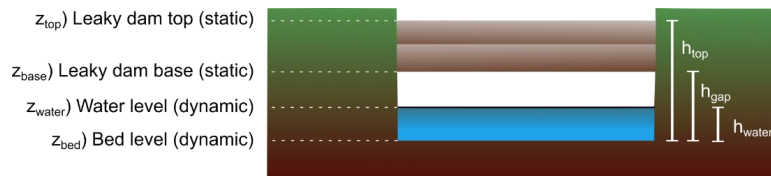
125 The approach developed herein represents the leakiness of a LD, its water depth-dependent impact on the water
column, and changing efficacy due to implicit geomorphic changes. It allows the simulation of gaps below LDs,
a common design feature, in a way that can alter due to erosion or deposition. In addition, the user can specify an
install time within the simulation timeline, thus allowing the model to reach steady state without LDs impacting
hydro- or morphodynamics. LDs can then be inserted into evolved landscapes, allowing a range of experimental
130 simulations that more realistically simulate LD installation.

The LD function uses a dynamic value for Manning's n roughness (henceforth n) for cells that have been assigned
as containing a LD. This method is straightforward to apply within a model domain, as specific cells can be
identified to place the LD in combination with other roughness variables such as in-channel or floodplain
135 boundary roughness (Liu et al., 2004; Kitts, 2010; Odoni and Lane, 2010; Dixon et al., 2016; Pinto et al., 2019;
Rasche et al., 2019; Barnsley, 2022; Senior et al., 2022). Roughness values can be determined from field
observations and utilised in numerical models (Shields and Gippel, 1995; Curran and Wohl, 2003; Kitts, 2010;
Dixon, 2013) but careful consideration of the application and transferability of roughness values between field
sites and at different scales must be considered, especially in steep river channels where higher roughness has less
140 impact compared to a physical blockage (Addy and Wilkinson, 2019). There is currently no implementation of a
stage-dependent dynamic roughness value for LDs in the literature. This is an important limitation of previous
approaches, since the relationship between flow resistance and LDs is known to be stage dependent (Jeffries et
al., 2003; Keys et al., 2018; Addy and Wilkinson, 2019; Muhawenimana et al., 2023). Senior et al. (2022) highlight
that care must be taken when interpreting the effectiveness of changing roughness values as it can slow the flow
145 of water rather than discretely store it. The approach adopted herein emulates the behaviours often observed by
LDs, but does not account for the entire hydraulic complexity as observed in laboratory studies (e.g.,
Muhawenimana et al., 2021).

The function applied herein determines the value of n to be used to estimate flow through each cell containing a
150 LD according to the proportion of the water column behind the LD that is in contact with the LD at each timestep.
If there is no LD, or the activation criteria are not met, n defaults to the default bed roughness defined by the user,
 n_{global} . Otherwise, a unique roughness, n_{local} is calculated for each timestep for each LD up to a maximum user
defined value (n_{max}). Adjustment to n is performed as a function of cell properties (see Figure 1): the initial



elevation of the bed (z_{bed}); current bed elevation upstream of the LD (z_{USbed}); and elevation of upstream water
 155 level (z_{water}). In addition, there are three user-defined properties: 1) the size of the vertical gap between the river
 bed and the base of the LD on installation, h_{gap} ; 2) the distance between the bed elevation at the start of the
 simulation and the top of the LD, h_{top} ; and 3) the maximum value of n if the entire water column upstream of the
 LD is in contact with it, n_{local} .
 CL employs first order upwinding. Therefore, for $cell_{xy}$, the model will calculate elevation values from the cell
 160 upwind of the LD from where water originates and the LD is assumed to take effect on the face between cells.
 The hydraulic model within CL uses the four cardinal neighbours (D4) to transport water and sediment, therefore
 only connected grid cells can transport material (O’Callaghan and Mark, 1984), resulting in no diagonal
 connections, as with the D8 flow direction algorithm. As such, for cell properties, the x and y coordinates can
 vary based on flow direction: $property_x = cell_{xy} | cell_{x-1,y}$, depending on which has the greatest water level
 165 in the x direction, and $propetry_y = cell_{xy} | cell_{x,y-1}$ for the y direction.



170 **Figure 1: Schematic showing hypothetical cross-sections for LD-containing cells. Elevations are represented as z_n and heights relative to z_{bed} as h_n . The LD becomes effective once the elevation of the water level (z_{water}) exceeds the elevation of the bottom of the LD (z_{base}). Throughout simulations, the elevations (z_{base} and z_{top}) expressing the absolute top and bottom elevations of the LD do not change so changes to the elevations of the water level (z_{water}) and the bed level (z_{bed}) will change its efficacy.**

There are two different methods of assigning a cell as containing a LD. The first method uses codes with each cell
 175 assigned a value between 0 and 5. If it is 0 there is no LD, if it is greater than 0, the cell is assigned one of five
 user-determined LD parameters, including a gap size (h_{gap}), height (h_{top}), and maximum roughness. Upon
 initialisation, the model will convert those parameters into z_{base} , z_{top} , and n_{max} . Additionally, the module
 determines the upstream direction and automatically assigns the LD to the corresponding cell face as shown in
 Figure 2. This enables the LD to be placed without considering flow direction.

180

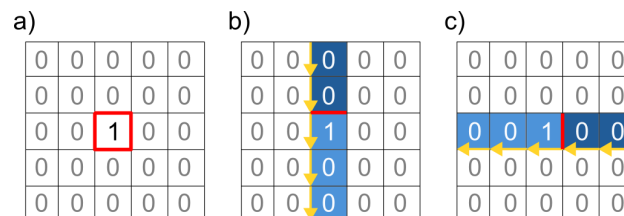


Figure 2: Leaky dam representation on a regular grid where 1 denotes an LD. Red shows the potential location for the LD along a cell face, yellow the flow direction between cells and blue relative water depth with a darker colour denoting deeper water. The location of the LD changes with flow direction. A) zero flow, therefore the LD could be on any cell



185 **face; B) flow from North to South, therefore the LD is on the Northern cell face; C) flow from East to West, therefore the LD is on the Eastern cell face.**

When the model is initialised, for each timestep the LD module will run through an iterative process, represented by Equation (1), that will determine the proportion of the LD in contact with the water column and calculate the scale of n using a blockage ratio (BR). If the LD is overtopped, there is less of the LD in contact with the water column, therefore n is reduced. Equally if the LD is not at maximum capacity, that is $h_{water} = h_{top}$, n will be scaled to less than n_{max} accordingly. The global Manning's value (n_{global}) is then combined with the scaled n_{max} to create n_{local} as shown in Equation (2) which is used in subsequent processing steps by CL.

$$1) \quad BR = \max\left(\frac{\min(z_{water}, z_{top}) - \max(z_{base}, z_{bed})}{h_{water}}, 0\right)$$

$$2) \quad n_{local} = n_{global}(1 - BR) + n_{max}BR$$

195

The proposed depth-weighted roughness representation method enables the user to emulate real-world implementations of LDs. Roughness (or porosity) quantification for structures such as LDs is often impractical at a large scale due to the required resolution of remotely sensed data, as well as the characteristics of the LD itself—geometry, litter cover, sorting, and wood size for example (Dixon, 2016; Livers et al., 2020). As such, the method represents a range of values that can be used to assess the extent of flow restriction caused by an LD and its relative impacts.

200

3. Methods

Prior to evaluating the impact of LDs on the hydrogeomorphology, sensitivity tests were conducted to understand the relationship between DEM grid resolution and the impact of simulating sediment transport compared to only the hydraulic component. Sensitivity analysis was performed using a single rainfall input—a six-hour, 0.1 annual exceedance probability (AEP) event—derived from the flood estimation handbook (Stewart et al., 2013) on a synthetic DEM (herein referred to as DEM_T).

205

3.1. Synthetic reach-scale terrain

The model domain was 160 m long and 100 m wide. The DEM had the same average slope as a prototype site (0.01 m m⁻¹; Wolstenholme, 2023) and was created by linear interpolation between the high and low survey points in the reach captured with a Topcon OS-103 Total Station (TS). DEM_T was resampled preserving minimum elevations to DEM_{Tj} where j represents the cell resolution (of either 1, 2 or 4 m as part of the grid sensitivity tests), ensuring channel depth and slope angle were preserved. To assess the influence of DEM resolution on model behaviour, a 1 m-deep, 4 m-wide channel was burnt into all DEMs.

210

3.2. Model set-up

A nested approach was used to drive model experiments at the reach scale. First, to derive discharge and sediment input for the reach of interest, discharge from the wider upper catchment, DEM_C (obtained from OS Terrain 5 data

215



at 5 m resolution; Ordnance Survey, 2020), was modelled using an extract of radar rainfall observations derived from the UK NIMROD radar network record for 2006–2020 (Met Office, 2003). This was applied at a 60-minute timestep to DEM_C as a global rainfall input to spin up the model and remove initial sediment extremes exported from the system due to an initial condition of homogenous grain size distributions across the DEM. This ensured that sediment types were distributed throughout the catchment in equilibrium with the topography. This was then repeated to derive a hydraulic and sediment flux input for the reach scale model.

The input grain size distribution was calculated using field data from Wolstenholme (2023). The site from which the grain size distribution was collected was approximately 2 km downstream of the LD, because LDs had been installed prior to surveying as the channel grain size distribution in the reach of interest would not be representative of a pre-LD scenario. The b-axis of >400 randomly selected clasts were measured from four locations in the reach, and the distributions binned into the nine default classes, as used by CL (see Figure 3). The grain size distribution was found to have a D_{50} of 12.8 mm, which was applied globally across the modelled reach domain. Within the model no sediment was transported in suspension and the Wilcock and Crowe (2003) sediment transport law was selected within CL since it was developed using a mixture of both sand and gravels, which is appropriate for the grain sizes used.

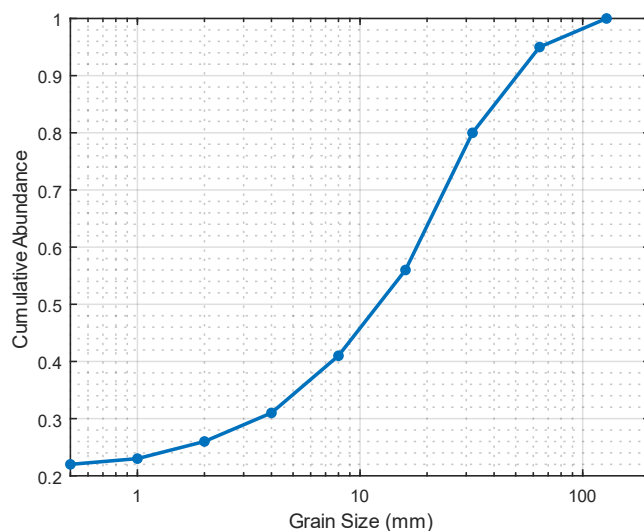


Figure 3: Grain size distribution used in experiments from Wolstenholme (2023).

3.3. Experimental design

Each DEM_{Tj} had a single LD installed 100 m downstream of the model input to assess geomorphic effects surrounding the LD and reduce potential impact from the model boundaries. A single rainfall storm was used (0.1 AEP with a six-hour rainfall duration) nested within a 120-hour period of baseflow. An initial period of 33.3 hours was used to fill the river reach and establish a hydraulic equilibrium, followed by the input to the reach model of a catchment-derived storm for a further 50 hours, then baseflow for the remainder of the run. The storm input was appended onto the spin-up period to ensure that all experiments that involved sediment transport had identical



initial conditions. The LD was “installed” following the spin period, 33 hours prior to the onset of the storm used for analysis. This allowed the river channel to adjust to baseflow without being impacted by the LD. Two LD gap variants were tested in each scenario (0 m and 0.2 m), and the maximum roughness (n_{max}) of the dams was set to 0.16.

LD height and width was constant throughout the experiments (0.5 m above initial channel bed, 4 m wide). Output data from the simulations, which provided information on outlet discharge, sediment yield for each grain size and total sediment yield, was recorded at a one-minute timestep. All tests were repeated with CLs ‘flow only’ option. When on, the erosion and deposition modules of the model are bypassed, and it functions as a 2D hydraulic model with a rigid boundary, as such hydraulic simulations were started 30 days prior to the onset of the storm. To assess the impact of the LDs on the system, the difference in peak discharge and storage capacity over time were calculated, comparing the cumulative discharge for a given storm to a corresponding ‘no LD’ baseline scenario. Finally, the influence of changing LD roughness and gap size was assessed.

4. Results

4.1. Model domain outputs

The influence of the LD on the model domain outputs was assessed through comparing the baseline (no LD scenario) to each of the LD variation experiments after the spin period, measured from the outlet of the model. Hydraulic-only simulations were more stable than the sediment transport enabled counterparts as shown in Figure 4. When $h_{gap} = 0$, hydraulic-only experiments show discharge attenuation of up to 1% when the LD is installed and further attenuation of up to 2.4% on the rising limb of the storm, before increasing ΔQ to 3.1% during the peak. When $h_{gap} = 0.2$, instantaneous discharge attenuation is not seen when the LD is installed, but the LD did increase discharge on the rising limb and the peak by up to 3%, before attenuating Q on the falling limb for both higher DEM resolutions, but reduced flows when a 1 m grid cell size is used (Figure 4).

In contrast, when sediment transport was enabled ΔQ contained substantially more variability after the storm. There was instant attenuation of up to 50% when $h_{gap} = 0$, for 2 m and 4 m DEM resolutions, and also up to 50% attenuation during the storm (see Figure 4C). In contrast, when $h_{gap} = 0.2$, there was no reduction in Q upon LD installation as seen in the equivalent hydraulic-only scenario, and reduction in Q of up to 4.7% for the 4 m DEM during the rising limb. For all sediment transport enabled experiments, the falling limb of the storm and remainder of the simulation time shows up to 25% deviation from the baseline scenario due to Q becoming out of phase with the baseline. This change represents a deviation in Q of up to $0.014 \text{ m}^3\text{s}^{-1}$ as a result of sediment transport and the presence of the LD.

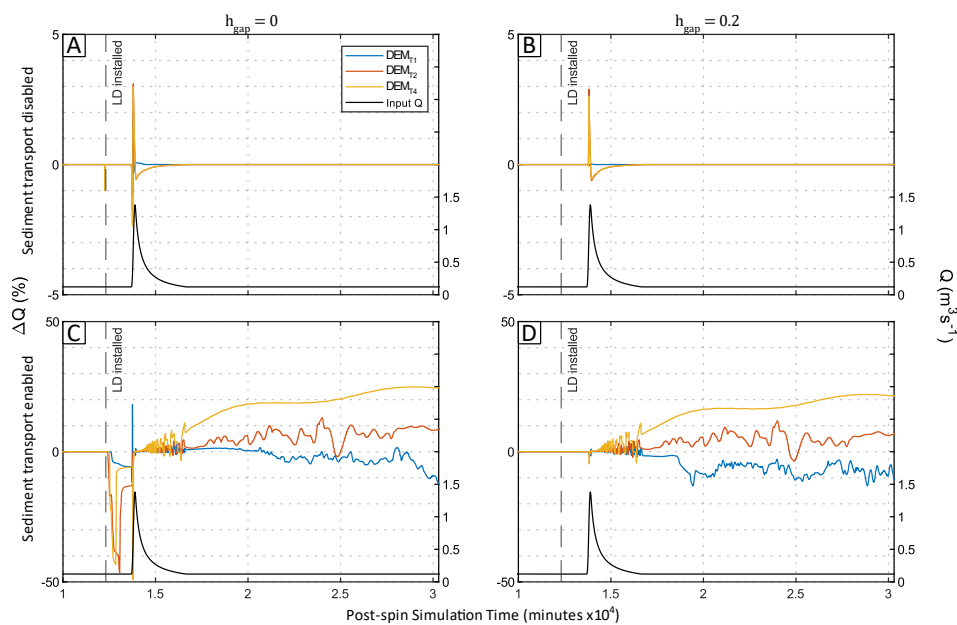


Figure 4: Impact of DEM grid resolution on predicted Q for sediment transport disabled/enabled experiments with LD gap size set to 0 m (A, C) or 0.2 m (B, D). Black line denotes input discharge (right axis, uniform across all experiments).

280 The impact on Q_s was determined using the same approach for Q detailed previously, but by comparing the
 cumulative Q_s rather than instantaneous flux. When the LD was installed, there was no impact on Q_s efflux of the
 model domain for any experiment. Across all the grid resolutions used, ΔQ_s was found to increase immediately
 following the peak of the storm and sediment was lost from the system. The 4 m grid resolution had a substantially
 larger sediment efflux (see Figure 5) when $h_{gap} = 0$ and to a lesser degree where $h_{gap} = 0.2$. On the falling limb
 285 and remainder of the simulation the 1 m and 2 m DEM resolutions had negative $\Delta \Sigma Q_s$ indicating that sediment
 efflux was lower than that of the baseline scenario and sediment is being stored in the reach. Although the 4 m
 resolution showed a similar behaviour, sediment efflux was continuously greater than the baseline.

290

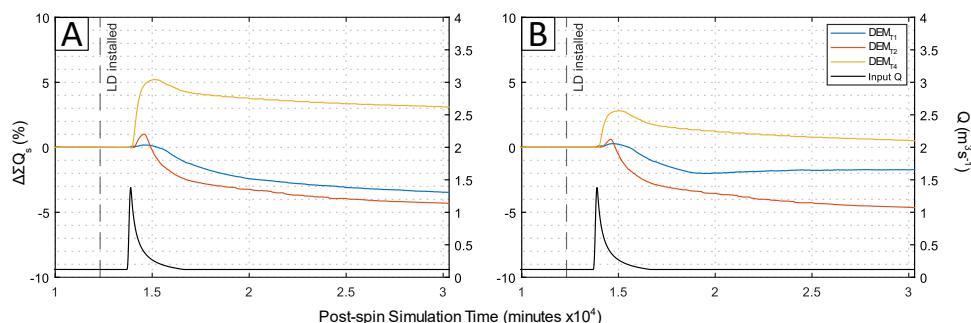
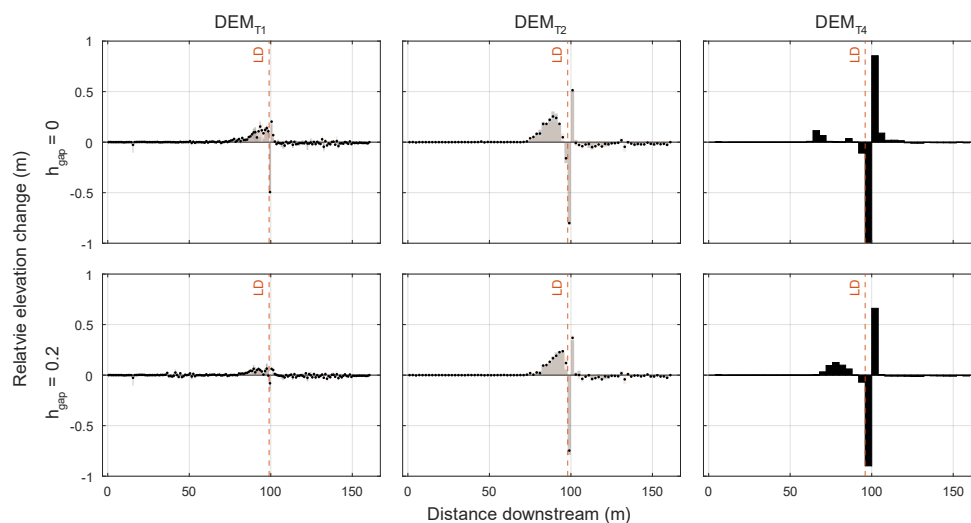


Figure 5: Cumulative ΔQ_s for 0 m LD gap (A) and 0.2 m gap (B) experiments. Input discharge shown for reference.

295 4.2. Geomorphological evolution

Geomorphological evolution was assessed within the model domain by comparing the average channel width elevation change to the baseline scenario for all experiments shown in Figure 6. Installing a single LD substantially influences bed elevation change throughout the system. All simulations with LDs had increased deposition 60–100 m downstream (average +0.12 m, maximum +0.25 m). The cell immediately upstream of the LD was typically erosive for DEM_{T4} when $h_{gap} = 0$ and 0.2 (0.07 and 0.11 m respectively). When the channel width was greater than one cell (i.e., DEM_{T1} & DEM_{T2}) there was also deposition predicted in the upstream cell of up to 0.12 m. Typically when $h_{gap} = 0.2$ there was less bed erosion predicted.

Immediately downstream of the LD had the most substantial bed elevation change, with all scenarios being highly erosive from -0.08 m (DEM_{T1}; $h_{gap} = 0.2$) to -0.99 m (DEM_{T4}; $h_{gap} = 0$). When $h_{gap} = 0$ there was more erosion in the downstream cell than when $h_{gap} = 0.2$. Downstream of the LD a depositional zone was predicted, with an elevation change similar in magnitude to the eroded cell upstream, ranging from 0.2–0.85 m (DEM_{T1}; $h_{gap} = 0.2$ and DEM_{T4}; $h_{gap} = 0$ respectively), and thus similarly there was more deposition where $h_{gap} = 0$. Overall, the order of magnitude and directionality of the elevation change is similar across all scenarios. Finally, for all scenarios following the second most cell downstream of the LD there was fluctuating propagation of bed elevation change predicted of the order of ± 0.10 m until the edge of the model domain.



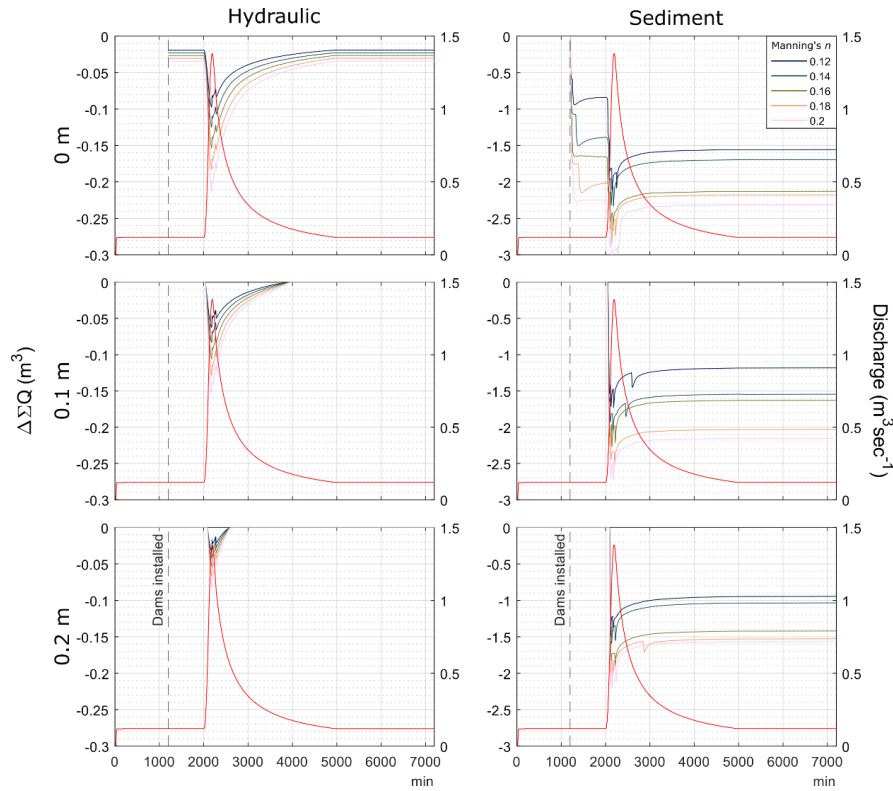
315 **Figure 6: Relative average channel bed elevation change for sediment transport enabled experiments. Bars show individual cell elevation change compared to the baseline scenario with the mean represented as a point for DEM_{T1} and DEM_{T2}.**

4.3. Leaky dam parameter adjustment

To explore the impact of varying n and the LD gap to build an envelope of potential responses, a 2 m DEM with a two-pixel wide channel (4 m) was chosen to use the highest resolution DEM that is practical to run across a suite of scenarios, whilst retaining a reasonable representation of the initial topography. Grain size, rainfall input and LD location were kept constant. Using the same hydraulic input as above, a no-LD baseline experiment was performed in addition to a matrix of 25 tests varying two LD parameters. First, the maximum LD roughness (n_{max}) was varied between 0.12–0.20 $s\ m^{-1/3}$ at intervals of 0.02 $s\ m^{-1/3}$. Values herein are based on empirical studies and are representative of naturally occurring log jams (Curran and Wohl, 2003; Dixon et al., 2016; Addy and Wilkinson, 2019). Second, the LD gap size was systematically varied from 0–0.4 m at 0.1 m intervals. Hydraulic and sediment transport enabled simulations were both performed, resulting in a total of 52 experiments.

4.3.1. Water storage

Sediment transport enabled simulations showed at least an order of magnitude greater water storage than the hydraulic equivalent. Where there was no LD gap, water was instantly stored upon LD installation until the onset of the storm where rougher LDs were found to store the greatest volume of water. Water storage is greatest during the peak of the storm and returns to baselevel immediately after the storm for hydraulic experiments, however when simulating sediment transport, the system stores 0.95–2.2 m^3 of water when compared to the baseline experiment, as shown in Figure 7.



335 **Figure 7: Water storage ($\Delta\Sigma Q$) for hydraulic and sediment transport enabled simulations, separated by LD gap size in metres. Manning's n ($s\ m^{-1/3}$) denoted in legend with input discharge represented in red. Note different y-axis scale.**

4.3.2. Sediment transport

Sediment transport was found not to be influenced by the installation of the LD, regardless of gap size (see Figure 8). During the storm there was a reduction in Q_s compared to the baseline scenario but there was little variability prior to the peak (average standard deviation: 0.008). Following the peak of the storm, the influence of roughness variability was more pronounced ($\Sigma\Delta Q_s$ 0.25–0.8 m^3), however there is no clear trend between the volume of sediment exiting the model domain (Figure 8) and the roughness used. However, increasing LD gap size did result in less sediment being lost out of the domain. Following the storm, sediment flux was lower than the baseline scenario (except where n was 0.14 or 0.18 $s\ m^{-1/3}$ and there is no LD gap) with a maximum difference of 0.5 m^3 (where n is 0.16 and the LD gap is 0.2 m).

340
345

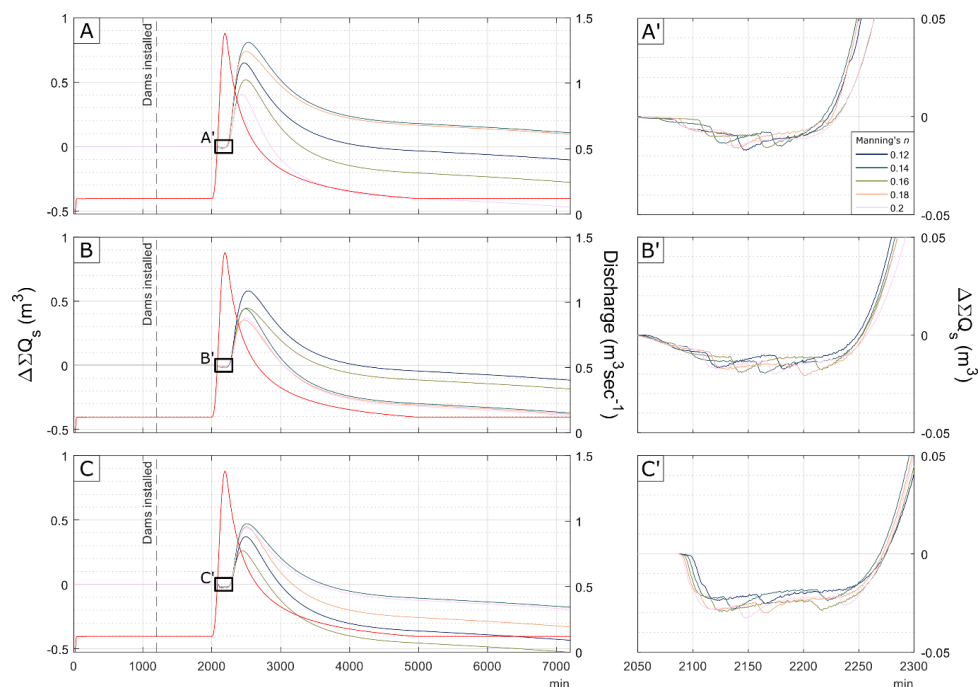
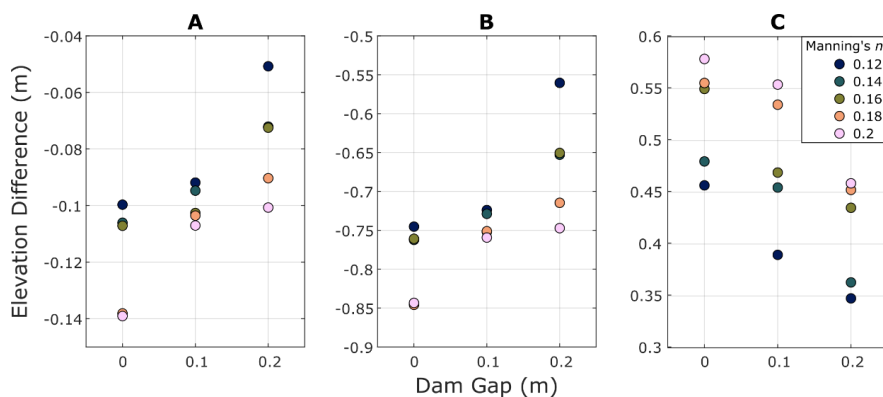


Figure 8: Cumulative sediment yield difference compared to the baseline scenario for 0, 0.1 and 0.2 m gap sizes (A–C respectively) separated by Manning’s n ($s\ m^{-1/3}$). Input discharge shown by red curve.

350 4.3.3. Elevation change

In section 4.24 it was shown that the LD mainly impacted the elevation of cells immediately upstream and downstream of the LD. As such, only these three sections of the channel were considered for localised bed elevation change analysis, as shown in Figure 9. Immediately upstream of the LD (Figure 9A) bed erosion magnitudes of 0.05–0.14 m were simulated, with a 0 m gap and high roughness (0.18–0.2 $s\ m^{-1/3}$) LD conditions, with lower volumes of erosion simulated with larger gap sizes and lower roughness values. There is a non-linear relationship between these parameters, with erosion magnitudes decreasing rapidly for higher roughness values as gap size increases, yet not as rapidly with lower roughness values applied. For example, where the LD gap is 0.1 m, erosion magnitudes are more closely clustered (0.105–0.092 m) than for other gap sizes. Zones immediately downstream of the LD (Figure 9B) experienced the most erosion, with up to 0.85 m of scour. The patterns and relative levels of bed erosion closely matches that of the zones immediately upstream of the LD, however at a greater orders of magnitude. Finally for the second cell downstream (i.e., 4 m from the LD), there is only deposition predicted (0.35–0.57 m). Higher roughness values experienced greater levels of deposition, which also decreased with increasing gap size.

355
360



365 **Figure 9: Elevation change for the cell immediately upstream of the LD (A), immediately downstream (B) and 4 m downstream (C) separated by Manning's n ($s\ m^{-1/3}$).**

5. Discussion

5.1. The CAESAR-Lisflood model

The results presented above demonstrates how CL can effectively represent LDs by dynamically adjusting localised Manning's n roughness values whilst accounting for different LD heights and gap sizes as a function of the proportion of the water column upstream of the LD. Placement of LDs is straightforward and can be achieved using a geographic information system, or through creation of a regular grid file, and simulations can be achieved using minimal data—a DEM, hydraulic input, and sediment GSD—to produce an overview of how a reach responds to LD installation. CL can therefore be used to aid identification of the ideal locations for LDs throughout a given reach to achieve the desired behavioural response, such as increased flow attenuation or enhanced geomorphic diversity. Through developing the ability to install a LD after a river channel has evolved to baseflow conditions, the simulation, and its output, are less affected by the bias of having these structures installed from the start of the simulation. As such, LDs are generated after baseflow has been established, which is more representative of the real LD installation process where wood is often felled and then anchored *in situ* while the river is flowing (Grabowski et al., 2019; Lo et al., 2021).

The effect of LDs—as well as natural log jams—is known to be stage dependant (Jeffries et al., 2003; Keys et al., 2018; Addy and Wilkinson, 2019; Muhawenimana et al., 2023), therefore it is important to ensure that the model can account for Manning's n being variable. Development of the LD module introduced above in CL builds upon previous work outlined by others (Dixon et al., 2016; Addy and Wilkinson, 2019; Hankin et al., 2020; Pearson, 2020; Walsh et al., 2020; Hill et al., 2023), filling a research gap through provision of a tool capable of generating dynamic roughness values that ensure that temporal variability in the stage-dependent LD-water relationship is captured. In addition, as CL utilises a regular raster grid, the required resolution can be adapted based on user requirements as well as computational resource availability. CL is a reduced complexity LEM that is not designed to simulate complex high-resolution channel flows, rather larger reach- and catchment-scale change over longer durations. As CL has the capability to simulate high-resolution environments (both spatially and temporally) at increased computational expense, it is important to recognise the impact of cell size throughout simulations.



However it is also important to note in the simulations presented above that the order of magnitude of predicted change was similar, regardless of model cell size, for water storage, geomorphology and discharge.

395

High-resolution cell sizes are the most computationally expensive. Increasing spatial resolution from two metres to one metre results in a four-fold increase in the number of cells that occupy the same extent, with almost double the number of model iterations. The increase in iterations is also dependent on the area that water interacts with, and the impact the water has on those cells. When simulating the impact of LDs and sediment transport, there was a two-fold increase in number of iterations compared to a no-LD scenario at all resolutions tested. In addition, higher resolution cell sizes (such as two metres) without LDs performed a similar number of iterations to the five metre resolution experiments with LDs when simulating sediment transport. As such, scale has substantial consequences for future work when simulating large catchments, despite having minimal influence on discharge. Increasing cell size results in a decrease in the accuracy of the true topography as the landscape is smoothed (Schoorl et al., 2000; Claessens et al., 2005), therefore it is important to utilise as high a resolution of grid as practical, without compromising the quality of model outputs. Resampling the input DEM can lead to variable channel widths and therefore a vast difference in potential water storage, which can introduce a substantial amount of bias into the results if not considered. Due to this, CL should only be used to understand broad behaviours that might be representative of a reach or catchment to discern information of interest where a finer resolution is impractical, especially at larger scales.

410

Cell size also has an impact on predicted geomorphic evolution. Higher resolutions can capture smaller scale fluctuations in bed elevation. Nevertheless herein it was found that coarser resolutions were able to predict relative changes that were of similar magnitudes to those predicted for finer resolution grids. All simulations predicted scour immediately downstream of the LD followed by a zone of deposition, with the perturbation fluctuating in magnitude as the signal weakens distal to the LD. Skinner and Coulthard (2022) showed that in CL as DEM grid cell increases, the representation of the hydrological network can become degraded, and although the model recorded similar total sediment yields following a 30-year continuous time series over a 0.5 km² catchment, this was from fewer geomorphologically active events. In this study a single-thread linear channel is used to evaluate the behaviour of the LD without introducing more complex morphological change or alterations to flow characteristics, similar to a laboratory environment. As such, the findings of Skinner and Coulthard (2022) regarding connectivity do not apply here, however further testing is required to evaluate the impact of a longer time series on geomorphic evolution and LD efficacy.

415

420

LEMs are notorious for being difficult to validate due to the lack of availability and paucity of calibration data (Wong et al., 2021). Combined with many adjustable parameters and initial conditions, there is a high probability for model equifinality (Coulthard and Skinner, 2016; Hancock et al., 2016; Skinner et al., 2018; Skinner et al., 2020). It is, however, possible to treat the outputs from an LEM, such as CL, in more abstract perspectives and use the results to identify the influence of intrinsic variables and the addition of structures to a system. As such, care must be taken when extracting and interpreting data outputs and using appropriate metrics in order to capitalise on data produced (Skinner et al., 2018). When simulating sediment transport and recording the output with high temporal resolution, discharge contained sharp increases and decreases due to pulses of sediment being

425

430



suddenly mobilised within the system when the transport threshold was reached (as seen in Figure 4). Thus, water storage is perhaps a more useful mechanism for accessing the influence of LDs at this scale, especially without producing vast amounts of extra data. A direct comparison can be performed between simulations which indicate the total volume of water being stored in a system compared to a system without LDs installed. The same practice can be applied to sediment stored within the system and aligned with the output hydrograph.

5.2. Sensitivity considerations

For the simple reach DEM_T used in the sensitivity suite of experiments it is clear that finer resolution grids are more computationally expensive due to the number of cells to be processed, yet the LD module almost doubles this computational expense. Despite this, elevation change across the river profile follows a similar pattern regardless of grid resolution and also has the same order of magnitude and directionality of change as shown in Figure 6. Grid resolution when simulating LDs impacts both Q and Q_s through increasing the effectiveness of Q reduction for both hydraulic and sediment transport enabled experiments. The activation of the LD also varied by up to 40 minutes depending on grid resolution. When simulating sediment transport, Q is substantially noisier than hydraulic only simulations, most likely due to CL reaching the threshold required to transport sediment. The noise in the data must also be considered when analysing simulation outputs, however, this may also be a function of the high temporal resolution output recording. Averaging sediment transport data to a lower temporal resolution (e.g., hourly) results in smoother outputs, at the cost of temporal detail. An alternative measure, water storage, calculated as the difference between cumulative Q for both the baseline and the LD implementation simulations may provide additional clarity on the broad impact of LD interventions. Additionally, Q_s and sediment storage is drastically different when increasing grid resolution from 2 m to 4 m, resulting in a five-fold increase in sediment efflux.

Care must be taken when using the LD module for CL as the right results, such as elevation change and Q reduction, may be overestimated when using coarser grid resolutions. CL should be used heuristically to mitigate these issues to best understand the impact of LDs in more complex and larger settings, focusing on the behaviouralist response of the reach or catchment to LD parameters and thus gain understanding for potential impacts rather than for predictive purposes.

5.3. Implications

Typically, for FRM, interventions are designed to reduce the risk of a specific flood event threshold derived from historic empirical data within a catchment. The effectiveness of an FRM structure in reducing the impacts of a given AEP is established through rigorous hydraulic modelling of different dimensions of the flow and structure, however modelling must be proportionate to the project considered (Environment Agency, 2022). The results herein show that understanding the influence of an FRM intervention on sediment transport is vital as geomorphic forcing resulting from a structure enables the estimation of the efficacy of an intervention for a catchment. Sediment transport becomes increasingly important when unintended geomorphic adjustment to 'hard engineered' structures can have reduce efficacy and potentially promote flooding downstream due to geomorphic change over time (Hesselink et al., 2003; Pinter et al., 2006; Hudson et al., 2008; Benito and Hudson, 2010). Utilising an understanding of both historic and present geomorphic changes to structures enables geomorphologists to inform



FRM strategies (Arnaud-Fassetta et al., 2009). Indeed, without understanding the geomorphic consequences, flood mitigation interventions have the potential to do more harm than good.

475 Channel evolution alongside LD interventions must be considered for both single storm events and long-term simulations due to the observations identified above. An LD fixed *in situ* can have a substantial effect on the hydrological regime as well as the boarder geomorphology of the river channel, which can, in turn, influence outcomes of flood risk modelling. Often, numerical modellers omit geomorphological process—especially at the event scale—for increased computational efficiency as they are considered to not have an impact greater than that of the uncertainties already present within the model (Flack et al., 2019), yet impounding a channel with an LD
480 can cause substantial geomorphological evolution from a single event alone.

It has been shown that modelling sediment transport can have an impact on the total volume of water that a reach is able to store compared to modelling hydraulics alone. It is important to therefore consider how modelling these processes can further inform future works, such as placement of LD interventions throughout a catchment, as well
485 as how best to utilise these resources to effectively identify locations for river restoration projects. Additionally, numerical modellers can utilise the LD module in CL from minutes, event-scale, annual, decadal and greater if desired, customising the outputs to the users' needs. CL has the capability to save an elevation file (amongst many others) at a given timestep, which could further the understanding of how these structures evolve throughout a storm or rainfall sequence.

490 The results herein suggest that practitioners should carefully consider the LD gap size as well as roughness of the intervention when installing the structure. Results here show that there is little impact on peak discharge for a single LD in a linear system, however the LDs used here are not designed to engage with the floodplain, and it is therefore not utilised. Larger gap sizes activate later in the storm, therefore may be used as a flood delay system
495 to only capture high flows above a certain height, with careful understanding of flow conditions where the LD is installed. Furthermore, adding more roughness elements to the LD increased potential water storage. The CL tool here uses roughness on a relative scale to provide insight into the impact of a rougher and less rough structure. Roughness can be combined with gap size to produce a similar effect, for example for DEM_{T2} , a $h_{gap} = 0.1$ and where $n_{max} = 0.14$ had a comparable and similar impact to conditions where $h_{gap} = 0.2$ and $n_{max} = 0.2$ on
500 downstream deposition. The implementation of dynamic roughness also advances simple LD representation in numerical models, particularly when exploring multi-LD reach and catchment-scale scenarios.

Natural flood management practitioners could also utilise the CL NFM tool to provide an understanding of how installing a given number of LDs may impact their reach and/or catchment of interest to develop a “big picture”
505 overview of their effectiveness for their given application such as, for example, sediment management, flood risk reduction, or habitat development. Numerical modelling should be used in conjunction with field studies to evaluate the potential effectiveness and cost-benefit analysis of the installation of multiple NFM interventions such as LDs. By enabling researchers and practitioners to easily implement LDs into CL, upper and lower boundaries of the potential impact of installations could be calculated and integrated into different climate
510 scenarios if required. CL presents an opportunity to achieve this with minimal data requirements, so long as the



user understands that the output should be regarded as a tool to investigate behaviour of the system and not forecasting the definite impact of LDs or other NFM interventions on a river system.

6. Conclusions

This study incorporated leaky wooden dams (LDs) into a numerical model capable of simulating both the hydrology and the sediment transport efficiently at the reach scale. The model also has scope to expand to the catchment-scale whilst simulating multiple complex storm events. The approach used herein has shown that it is important to consider sediment transport and morphological evolution when numerically modelling leaky dams, even at event scale. This is because of the impacts this has on altering the total volume of water stored by the LDs, in addition to inducing greater geomorphological complexity. Based on a synthetic DEM, LD gap size was shown to be much more important than dam roughness when numerically modelling with the CL method and could be utilised in the future by NFM practitioners looking to install similar structures within a reach and/or catchment. The study also highlights the need to correctly represent a gap in LD models, as well as the need to consider adopting a behavioural approach to the numerical modelling of such structures.

7. Author contributions

JW and CS conceived the study and designed the experiments. CS added the LD module into CAESAR-Lisflood codebase. JW performed the simulations, data analysis and writing of the first draft. JW, CS, DM, RT and DP equally contributed to discussing and interpreting the results and finalising the draft.

8. Code and data availability

The current version of CAESAR-Lisflood is available from <https://sourceforge.net/projects/caesar-lisflood/files/> under the GNU General Public Licence version 3.0 (GPLv3).

The exact version of the model used to produce the results using in this paper are archived used Zenodo and available at <https://doi.org/10.5281/zenodo.12795495>, as are input data and scripts to run the model for simulations presented in this paper.

9. Competing interests

The corresponding author has declared that none of the authors have any competing interests.

10. References

Addy, S., and Wilkinson, M. E.: An assessment of engineered log jam structures in response to a flood event in an upland gravel-bed river, *Earth Surface Processes and Landforms*, 4112, 1658–1670. <https://doi.org/10.1002/esp.3936>, 2016.



- Addy, S., and Wilkinson, M. E.: Representing natural and artificial in-channel large wood in numerical hydraulic and hydrological models, *WIREs Water*, 6, 1–20, <https://doi.org/10.1002/wat2.1389>, 2019.
- Arnaud-Fassetta, G., Astrade, L., Bardou, É., Corbonnois, J., Delahaye, D., Fort, M., Gautier, E., Jacob, N., Peiry, J.-L., Piégay, H., and Penven, M.-J.: Fluvial geomorphology and flood-risk management, *Géomorphologie: Relief, Processus, Environnement*, 152, 109–128. <https://doi.org/10.4000/geomorphologie.7554>, 2009.
- 545 Bair, R. T., Segura, C., and Lorion, C. M.: Quantifying restoration success of wood introductions to increase Coho salmon winter habitat, *Earth Surface Dynamics*, 73, 841–857, <https://doi.org/10.5194/esurf-2019-10>, 2019.
- Barnsley, I.: Quantifying the benefits of natural flood management methods in groundwater-dominated river systems, Ph.D. thesis, University of Southampton, 219 pp., 2022.
- 550 Bates, P. D., Horritt, M. S., and Fewtrell, T. J.: A simple inertial formulation of the shallow water equations for efficient two-dimensional flood inundation modelling. *Journal of Hydrology*, 3871–2, 33–45, <https://doi.org/10.1016/j.jhydrol.2010.03.027>, 2010.
- Benito, G., and Hudson, P. F.: Flood hazards: The context of fluvial geomorphology. In A.-A. Irasema and A. S. Goudie Eds., *Geomorphological Hazards and Disaster Prevention* pp. 111–128. Cambridge University Press, <https://doi.org/10.1017/CBO9780511807527.010>, 2010.
- 555 Burgess-Gamble, L., Ngai, R., Wilkinson, M., Nisbet, T., Pontee, N., Harvey, R., Kipling, K., Addy, S., Rose, S., Maslen, S., Jay, H., Nicholson, A., Page, T., Jonczyk, J., and Quinn, P.: Working with Natural Processes-Evidence Directory SC150005, <https://www.gov.uk/government/organisations/environment-agency/about/research>, 2017.
- Cashman, M. J., Wharton, G., Harvey, G. L., Naura, M., and Bryden, A.: Trends in the use of large wood in UK river restoration projects: insights from the National River Restoration Inventory, *Water and Environment Journal*, 33Ea 2017, 318–328, <https://doi.org/10.1111/wej.12407>, 2018.
- 560 Claessens, L., Heuvelink, G. B. M., Schoolt, J. M., and Veldkamp, A.: DEM resolution effects on shallow landslide hazard and soil redistribution modelling, *Earth Surface Processes and Landforms*, 304, 461–477, <https://doi.org/https://doi.org/10.1002/esp.1155>, 2005.
- 565 Coulthard, T. J., and Skinner, C. J.: The sensitivity of landscape evolution models to spatial and temporal rainfall resolution, *Earth Surface Dynamics*, 43, 757–771, <https://doi.org/10.5194/esurf-4-757-2016>, 2016.
- Coulthard, T. J., Neal, J. C., Bates, P. D., Ramirez, J., de Almeida, G. A. M., and Hancock, G. R.: Integrating the LISFLOOD-FP 2D hydrodynamic model with the CAESAR model: Implications for modelling landscape evolution. *Earth Surface Processes and Landforms*, 3815, 1897–1906, <https://doi.org/10.1002/esp.3478>, 2013.
- 570 Croke, J., Fryirs, K., and Thompson, C.: Defining the floodplain in hydrologically-variable settings: implications for flood risk management, *Earth Surface Processes and Landforms*, 4114, 2153–2164, <https://doi.org/10.1002/esp.4014>, 2016.
- Curran, J. H., and Wohl, E. E.: Large woody debris and flow resistance in step-pool channels, Cascade Range, Washington, *Geomorphology*, 511, 141–157, <https://doi.org/https://doi.org/10.1016/S0169-555X0200333-1>, 2003.
- 575 Dadson, S. J., Hall, J. W., Murgatroyd, A., Acreman, M., Bates, P., Beven, K., Heathwaite, L., Holden, J., Holman, I. P., Lane, S. N., O’Connell, E., Penning-Rowsell, E., Reynard, N., Sear, D., Thorne, C., Wilby, R., Connell, E. O., Reynard, N., and Sear, D.: A restatement of the natural science evidence concerning flood management in the UK, *Proceedings of the Royal Society*, 47320160706, <https://doi.org/http://dx.doi.org/10.1098/rspa.2016.0706>, 2017.
- 580



- Deane, A., Norrey, J., Coulthard, E., McKendry, D. C., and Dean, A. P.: Riverine large woody debris introduced for natural flood management leads to rapid improvement in aquatic macroinvertebrate diversity, *Ecological Engineering*, 163, <https://doi.org/10.1016/j.ecoleng.2021.106197>, 2021.
- Dixon, S. J., Sear, D. A., Odoni, N. A., Sykes, T., and Lane, S. N.: The effects of river restoration on catchment scale flood risk and flood hydrology. *Earth Surface Processes and Landforms*, 417, 997–1008, <https://doi.org/10.1002/esp.3919>, 2016.
- Dixon, S. J.: Investigating the effects of large wood and forest management on flood risk and flood hydrology, <https://doi.org/10.13140/RG.2.1.4923.2485>, 2013.
- Dixon, S. J.: A dimensionless statistical analysis of logjam form and process, *Ecohydrology*, 96, 1117–1129, <https://doi.org/10.1002/eco.1710>, 2016.
- Einstein, H. A.: The Bed-Load Function for Sediment Transportation in Open Channel Flows, In *Technical Bulletin No. 1026* pp. 1–31, US Department of Agriculture, 1950.
- Environment Agency.: *Flood and coastal erosion risk management appraisal: Technical guidance*, 2022.
- Feeney, C. J., Godfrey, S., Cooper, J. R., Plater, A. J., and Dodds, D.: Forecasting riverine erosion hazards to electricity transmission towers under increasing flow magnitudes, *Climate Risk Management*, 36, <https://doi.org/10.1016/j.crm.2022.100439>, 2022.
- Flack, D. L. A., Skinner, C. J., Hawkness-Smith, L., O'Donnell, G., Thompson, R. J., Waller, J. A., Chen, A. S., Moloney, J., Largeton, C., Xia, X., Blenkinsop, S., Champion, A. J., Perks, M. T., Quinn, N., and Speight, L. J.: Recommendations for Improving Integration in National End-to-End Flood Forecasting Systems: An Overview of the FFIR Flooding From Intense Rainfall Programme, *Water*, 114, <https://doi.org/10.3390/w11040725>, 2019.
- Grabowski, R. C., Gurnell, A. M., Burgess-Gamble, L., England, J., Holland, D., Klaar, M. J., Morrissey, I., Uttley, C., and Wharton, G.: The current state of the use of large wood in river restoration and management, *Water and Environment Journal*, 1–12, <https://doi.org/10.1111/wej.12465>, 2019.
- Gregory, K. J., Gurnell, A. M., and Hill, C. T.: The permanence of debris dams related to river channel processes, *Hydrological Sciences Journal*, 303, 371–381, <https://doi.org/10.1080/02626668509491000>, 1985.
- Hancock, G. R., Lowry J. B. C., and Coulthard, T. J.: Catchment reconstruction — erosional stability at millennial time scales using landscape evolution models, *Geomorphology*, 231, 15–27, <https://doi.org/10.1016/j.geomorph.2014.10.034>, 2015.
- Hancock, G. R., Verdon-Kidd, D., and Lowry, J. B. C.: Sediment output from a post-mining catchment – Centennial impacts using stochastically generated rainfall, *Journal of Hydrology*, 544, 180–194, <https://doi.org/10.1016/j.jhydrol.2016.11.027>, 2017.
- Hankin, B., Metcalfe, P., Beven, K., and Chappell, N. A.: Integration of hillslope hydrology and 2D hydraulic modelling for natural flood management, *Hydrology Research*, 506, 1535–1548, <https://doi.org/10.2166/nh.2019.150>, 2019.
- Hankin, B., Hewitt, I., Sander, G., Danieli, F., Formetta, G., Kretzschmar, A., Kiradjiev, K., Wong, C., Pegler, S., and Lamb, R.: A risk-based, network analysis of distributed in-stream leaky barriers for flood risk management, *Natural Hazards and Earth System Sciences*, 1–22, <https://doi.org/10.5194/nhess-2019-394>, 2020.
- Hesslink, A. W., Weerts, H. J. T., and Berendsen, H. J. A.: Alluvial architecture of the human-influenced river Rhine, The Netherlands, *Sedimentary Geology*, 161, 229–248, <https://doi.org/10.1016/S0037-07380300116-7>, 2003.



- Hill, B., Liang, Q., Boshier, L., Chen, H., and Nicholson, A.: A systematic review of natural flood management modelling: Approaches, limitations, and potential solutions, *Journal of Flood Risk Management*, 163, e12899, <https://doi.org/https://doi.org/10.1111/jfr3.12899>, 2023.
- Hudson, P. F., Middelkoop, H., and Stouthamer, E.: Flood management along the Lower Mississippi and Rhine Rivers (The Netherlands) and the continuum of geomorphic adjustment, *Geomorphology*, 1011–2, 209–236, <https://doi.org/10.1016/j.geomorph.2008.07.001>, 2008.
- Jeffries, R., Darby, S. E., and Sear, D. A.: The influence of vegetation and organic debris on flood-plain sediment dynamics: Case study of a low-order stream in the New Forest, England, *Geomorphology*, 511–3, 61–80, <https://doi.org/10.1016/S0169-555X0200325-2>, 2003.
- 625 Keys, T. A., Govenor, H., Jones, C. N., Hession, W. C., Hester, E. T., and Scott, D. T.: Effects of large wood on floodplain connectivity in a headwater Mid-Atlantic stream, *Ecological Engineering*, 118, 134–142, <https://doi.org/10.1016/j.ecoleng.2018.05.007>, 2018.
- Kitts, D. R.: The hydraulic and hydrological performance of large wood accumulation in a low-order forest stream, Ph.D. thesis, University of Southampton, pp.367, 2010.
- 635 Lane, S. N.: Natural Flood Management, *WIREs Water*, 4, 2017.
- Leakey, S., Hewett, C. J. M., Glenis, V., and Quinn, P. F.: Modelling the Impact of Leaky Barriers with a 1D Godunov-Type Scheme for the Shallow Water Equations, *Water*, 122, <https://doi.org/10.3390/w12020371>, 2020.
- Li, C., Wang, M., Chen, F., Coulthard, T. J., and Wang, L.: Integrating the SLIDE model within CAESAR-Lisflood: Modeling the ‘rainfall-landslide-flash flood’ disaster chain mechanism under landscape evolution in a mountainous area, *Catena*, 227, 107124, <https://doi.org/10.1016/j.catena.2023.107124>, 2023.
- 640 Liu, Y. B., Gebremeskel, S., de Smedt, F., Hoffmann, L., and Pfister, L.: Simulation of flood reduction by natural river rehabilitation using a distributed hydrological model, *Hydrology and Earth System Sciences*, 86, 1129–1140, <https://doi.org/10.5194/hess-8-1129-2004>, 2004.
- Livers, B., Lininger, K. B., Kramer, N., and Sendrowski, A.: Porosity problems: Comparing and reviewing methods for estimating porosity and volume of wood jams in the field, *Earth Surface Processes and Landforms*, 4513, 3336–3353, <https://doi.org/10.1002/esp.4969>, 2020.
- Lo, H. W., Smith, M., Klaar, M., and Woulds, C.: Potential secondary effects of in-stream wood structures installed for natural flood management: A conceptual model, *WIREs Water*, 85, <https://doi.org/10.1002/wat2.1546>, 2021.
- Meadows, T.: Forecasting long-term sediment yield from the upper North Fork Toutle River, Mount St. Helens, USA, Ph.D. thesis, University of Nottingham, pp.393, 2014.
- Met Office.: Met Office Rain Radar Data from the NIMROD System, NCAS British Atmospheric Data Centre, <http://catalogue.ceda.ac.uk/uuid/82adec1f896af6169112d09cc1174499>, 2003.
- Metcalfe, P., Beven, K., Hankin, B., and Lamb, R.: A modelling framework for evaluation of the hydrological impacts of nature-based approaches to flood risk management, with application to in-channel interventions across a 29-km² scale catchment in the United Kingdom, *Hydrological Processes*, 319, 1734–1748, <https://doi.org/10.1002/hyp.11140>, 2017.
- 655 Meyer-Peter, E., and Müller, R.: Formulas for Bed-Load Transport, Paper No. 2, Proceedings of the 2nd Congress, IAHR, 39–64, 1948.
- Muhawenimana, V., Wilson, C. A. M. E., Nefjodova, J., and Cable, J.: Flood attenuation hydraulics of channel-spanning leaky barriers. *Journal of Hydrology*, 596, 125731, <https://doi.org/10.1016/j.jhydrol.2020.125731>, 2021.
- 660



- Muhawenimana, V., Follett, E., Maddock, I., and Wilson, C. A. M. E.: Field-based monitoring of instream leaky barrier backwater and storage during storm events. *Journal of Hydrology*, 129744, <https://doi.org/10.1016/j.jhydrol.2023.129744>, 2023.
- Newson, M., Lewin, J., and Raven, P.: River science and flood risk management policy in England, *Progress in Physical Geography: Earth and Environment*, <https://doi.org/10.1177/03091333211036384>, 2021.
- 665 Nicholson, A. R., Wilkinson, M. E., O'Donnell, G. M., and Quinn, P. F.: Runoff attenuation features: A sustainable flood mitigation strategy in the Belford catchment, UK, *Area*, 444, 463–469. <https://doi.org/10.1111/j.1475-4762.2012.01099.x>, 2012.
- Nicholson, A. R., O'Donnell, G. M., Wilkinson, M. E., and Quinn, P. F.: The potential of runoff attenuation
670 features as a Natural Flood Management approach, *Journal of Flood Risk Management*, e12565, 1–14, <https://doi.org/10.1111/jfr3.12565>, 2019.
- O'Callaghan, J. F., and Mark, D. M.: The extraction of drainage networks from digital elevation data. *Computer Vision, Graphics, and Image Processing*, 283, 323–344, <https://doi.org/10.1016/S0734-189X8480011-0>, 1984.
- 675 Odoni, N. A., and Lane, S. N.: Assessment of the Impact of Upstream Land Management Measures on Flood Flows in Pickering Beck using Overflow, 2010.
- Ordnance Survey.: OS Terrain 5 DTM [ASC geospatial data], Scale 1:20000, Tiles: Dalby Forest, Updated: April 2020 Ordnance Survey, <http://digimap.edina.ac.uk/>, 2020.
- Pearson, E. G.: Modelling the interactions between geomorphological processes and Natural Flood Management. Ph.D. thesis, University of Leeds, pp.251, 2020.
- 680 Peleg, N., Skinner, C., Ramirez, J. A., and Molnar, P.: Rainfall spatial-heterogeneity accelerates landscape evolution processes, *Geomorphology*, 390, <https://doi.org/10.1016/j.geomorph.2021.107863>, 2021.
- Pinter, N., Ickes, B. S., Wlosinski, J. H., and van der Ploeg, R. R.: Trends in flood stages: Contrasting results from the Mississippi and Rhine River systems, *Journal of Hydrology*, 3313–4, 554–566,
685 <https://doi.org/10.1016/j.jhydrol.2006.06.013>, 2006.
- Pinto, C., Ing, R., Browning, B., Delboni, V., Wilson, H., Martyn, D., and Harvey, G. L.: Hydromorphological, hydraulic and ecological effects of restored wood: findings and reflections from an academic partnership approach, *Water and Environment Journal*, 333, 353–365, <https://doi.org/10.1111/wej.12457>, 2019.
- Ramirez, J. A., Zischg, A. P., Schürmann, S., Zimmermann, M., Weingartner, R., Coulthard, T., and Keiler, M.:
690 Modeling the geomorphic response to early river engineering works using CAESAR-Lisflood. *Anthropocene*, 32, 100266, <https://doi.org/10.1016/j.ancene.2020.100266>, 2020.
- Rasche, D., Reinhardt-Imjela, C., Schulte, A., and Wenzel, R.: Hydrodynamic simulation of the effects of stable in-channel large wood on the flood hydrographs of a low mountain range creek, Ore Mountains, Germany, *Hydrology and Earth System Sciences*, 2310, 4349–4365, <https://doi.org/10.5194/hess-23-4349-2019>, 2019.
- 695 Schoorl, J. M., Sonneveld, M. P. W., and Veldkamp, A.: Three-dimensional landscape process modelling: the effect of DEM resolution, *Earth Surface Processes and Landforms*, 259, 1025–1034, [https://doi.org/10.1002/1096-9837\(200008\)25:9<1025::AID-ESP116>3.0.CO;2-Z](https://doi.org/10.1002/1096-9837(200008)25:9<1025::AID-ESP116>3.0.CO;2-Z), 2000.
- Senior, J. G., Trigg, M. A., and Willis, T.: Physical representation of hillslope leaky barriers in 2D hydraulic models: A case study from the Calder Valley, *Journal of Flood Risk Management*, 153,
700 <https://doi.org/10.1111/jfr3.12821>, 2022.



- SEPA.: Natural Flood Management Handbook, 2015.
- Shields Jr., F. D., Gippel, C. J., Shields Jr., F. D., and Gippel, C. J.: Prediction of effects of woody debris removal on flow resistance, *Journal of Hydraulic Engineering*, 1214, 341–354, <https://doi.org/10.1061/ASCE0733-94291995121:4341>, 1995.
- 705 Skinner, C. J., and Coulthard, T. J.: The sensitivity of Landscape Evolution Models to DEM grid cell size. *Earth Surf. Dynam. Discuss.*, 2022, 1–26, <https://doi.org/10.5194/esurf-2022-30>, 2022.
- Skinner, C. J., Coulthard, T. J., Schwanghart, W., van de Wiel, M. J., and Hancock, G.: Global sensitivity analysis of parameter uncertainty in landscape evolution models, *Geoscientific Model Development*, 1112, 4873–4888, <https://doi.org/10.5194/gmd-11-4873-2018>, 2018.
- 710 Skinner, C. J., Peleg, N., Quinn, N., Coulthard, T. J., Molnar, P., and Freer, J.: The impact of different rainfall products on landscape modelling simulations, *Earth Surface Processes and Landforms*, 4511, 2512–2523, <https://doi.org/10.1002/esp.4894>, 2020.
- Stewart, E. J., Jones, D. A., Svensson, C., Morris, D. G., Dempsey, P., Dent, J. E., Collier, C. G., and Anderson, C. W.: Reservoir safety—Long return period rainfall, Department for Environment, Food and Rural Affairs, 2013.
- 715 Thomas, H., and Nisbet, T.: Modelling the hydraulic impact of reintroducing large woody debris into watercourses, *Journal of Flood Risk Management*, 52, 164–174, <https://doi.org/10.1111/j.1753-318X.2012.01137.x>, 2012.
- Walsh, P., Jakeman, A., and Thompson, C.: Modelling headwater channel response and suspended sediment yield to in-channel large wood using the Caesar-Lisflood landscape evolution model, *Geomorphology*, 363, 107209, <https://doi.org/10.1016/j.geomorph.2020.107209>, 2020.
- 720 Wenzel, R., Reinhardt-Imjela, C., Schulte, A., and Bölscher, J.: The potential of in-channel large woody debris in transforming discharge hydrographs in headwater areas Ore Mountains, Southeastern Germany, *Ecological Engineering*, 71, 1–9, <https://doi.org/10.1016/j.ecoleng.2014.07.004>, 2014.
- Wilcock, P. R., and Crowe, J. C.: Surface-based Transport Model for Mixed-Size Sediment, *Journal of Hydraulic Engineering*, 1292, 120–128, <https://doi.org/10.1061/ASCE0733-94292003129:2120>, 2003.
- 725 Wolstenholme, J.: Monitoring and modelling fluvial hydrogeomorphic response to leaky wooden dams, Ph.D. thesis, University of Hull, pp.227, 2023.
- Wong, J. S., Freer, J. E., Bates, P. D., Warburton, J., and Coulthard, T. J.: Assessing the hydrological and geomorphic behaviour of a landscape evolution model within a limits-of-acceptability uncertainty analysis framework, *Earth Surface Processes and Landforms*, 46, 2021.
- 730 Xie, J., Coulthard, T. J., and McLelland, S. J.: Modelling the impact of seismic triggered landslide location on basin sediment yield, dynamics and connectivity, *Geomorphology*, 398, <https://doi.org/10.1016/j.geomorph.2021.108029>, 2022.